

AD 709965

Quarterly Progress Report No. 5

Development of Nondestructive Tests for
the Evaluation of Bonded Materials

by

J. R. Zurbrick

1970 January 20 - 1970 April 19.

AVSD-0176-70-CR

Contract No. N00156-69-C-0913

Sponsored by

Advanced Research Project Agency
ARPA Order No. 1247 Amend. 1
Program Code No. 9D10

Submitted by

Avco Corporation
Avco Systems Division
Lowell, Massachusetts 01851

Reproduced by the
CLEARINGHOUSE
for Federal Scientific & Technical
Information Springfield Va 22151

Information
to be major

Approved
date; 11/1/70

I. INTRODUCTION

This report covers the work performed and the results obtained under the subject contract during the quarter 1970 January 20 through 1970 April 19. Data correlations and analyses for the Surface Condition Study are discussed. The basis for, and derivation of, an equation which provides the means to predict bond strength are presented. Results of feasibility studies for NDT techniques suitable to substrate surface characterization are discussed.

II. PROGRESS ACCOMPLISHED

A. Surface Condition Study

1. Data correlation and analysis

All of the data, notes, and photographs obtained during the Surface Condition Study were assembled according to specimen type and nominal surface roughness. The cosine values of all contact angles were obtained from trigonometric tables and added to the data lists. These lists served as the primary data source for crossplot trials.

The first reaction to the lists was one of frustration. The values gave the initial impression of complete and unrelated randomness. (Such is not unusual in adhesive bonding studies.) A few simple relations among three or perhaps four specimens were observed through casual inspection of the data, but these were promptly reversed by another set of specimens. Based on this, however, a number of computer analyses were run using linear equation solution for three unknowns, from data of three selected specimens. The equation format for this multifunctional, multivariable study was generally:

$$\text{Bond Strength} = (C_1)(1 + \cos \theta) + (C_2)(\text{CLA}) + C_3\left(\frac{1}{\text{thickness}}\right) \quad (1)$$

The experimental values were simultaneously solved together to provide empirical values for the linear constants, C_1 , C_2 , and C_3 . The format in equation (1) satisfied the general conclusions drawn in the adhesive bonding literature.

The general conclusion from the linear-equation trials was that the $\cos \theta$ term seemed to dominate the data, that inverse bondline thickness modified the relationship, and that CLA was of no consequence. The lack of correlation in CLA was expected (Reference 1). The other two observations satisfied the findings and conclusions most frequently found in the literature and most generally agreed to by adhesive bonding technologists (Reference 2).

The data analysis effort was shifted to direct concentration on the $\cos \theta$ interrelationships to seek out the primary single function involving bond strength. No direct relationship could be found between any of the four contact angle values (as prepared $\cos \theta$ max and $\cos \theta$ min; after-etch $\cos \theta$

max and $\cos \theta_{\min}$) and bond strength. The idea of historical influence was studied through these relationships:

$$\cos \theta_{\max} \text{ Ratio} = \frac{(1 + \cos \theta_{\max})_E - (1 + \cos \theta_{\max})_M}{(1 + \cos \theta_{\max})_E} \quad (2)$$

$$\cos \theta_{\min} \text{ Ratio} = \frac{(1 + \cos \theta_{\min})_E - (1 + \cos \theta_{\min})_M}{(1 + \cos \theta_{\min})_E} \quad (3)$$

where: subscripts, M = as prepared; E = after etch.

It was generally observed that the surfaces prepared with the smoother finishes were roughened by etching, and that those prepared with the rougher finishes were smoothed by etching. There appeared, through the ratios of equations (2) and (3), an impression that initial surface preparation did influence bond strength, even though considerable changes due to etching had taken place. No direct correlation of this, however, could be obtained.

Attention was then turned to bondline thickness as a function of bond strength. No direct correlation was observed. The misalignment of substrates was taken into consideration by observing the thickness variation of each bondline as well as its average thickness. Again, no support for a direct correlation to bond strength was forthcoming.

These experiences turned the attention to the bond strength values themselves. The questions, "how exactly were the values obtained for each type of specimen; what was considered in calculating bond strength (breaking load divided by ideal bonding area); and what measurement errors were inherent?" The answers, mostly speculative, shed no real light on the meaningfulness of the reported bond strength values.

One firm relationship did grow out of this study. It was observed that a brittle fracture pattern was exhibited by each of the butt tensile and core shear specimens, figures 1 and 2. An analogous pattern was somewhat evident in the lap shear specimens, figure 3.

The failure mechanism appeared to be as follows:

- a. Initiation of failure at the interface between cured adhesive and one of the substrates. ("adhesive failure")
- b. Brittle failure by rapid wavefront propagation radially away from the initiation site. Failure was "cohesive" in the cured adhesive.
- c. Breakup of the shock wavefront and subsequent dissipation of energy by scattering.
- d. Final separation of the bonded joint by non-brittle, viscoelastic flow, somewhat analogous to the peeling mechanism.

1 A&B

2 A&B

3 A&B



7 RMS NOMINAL, PAPER LAPPED



40 RMS NOMINAL, PAPER SANDED

1 A&B

2 A&B

3 A&B



FINE GRAIN, LOW PRESSURE GRIT BLAST



COARSE GRAIN, LOW PRESSURE GRIT BLAST

FIGURE 1. BOND FRACTURE SURFACES OF SELECTED BUTT TENSILE SPECIMENS

1 A&B

2 A&B

3 A&B



7 RMS NOMINAL, PAPER LAPPED



80 RMS NOMINAL, PAPER SANDED

1 A&B

2 A&E

3 A&B



110 RMS NOMINAL, TURNED



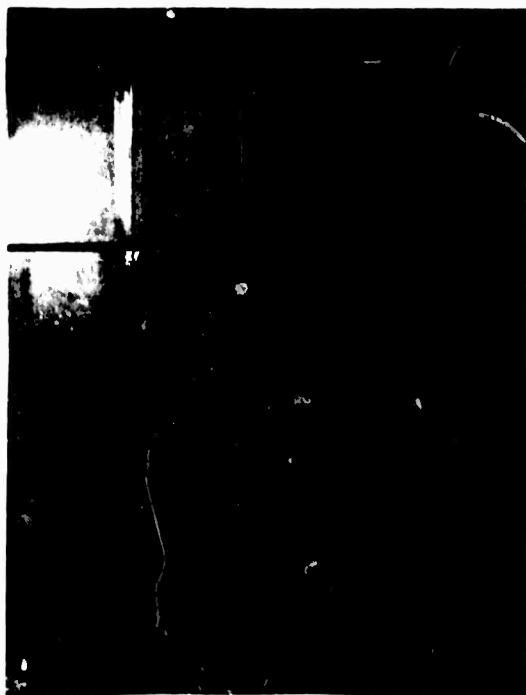
COARSE GRAIN, LOW PRESSURE GRIT BLAST

FIGURE 2. BOND FRACTURE SURFACES OF
SELECTED CORE SHEAR SPECIMENS

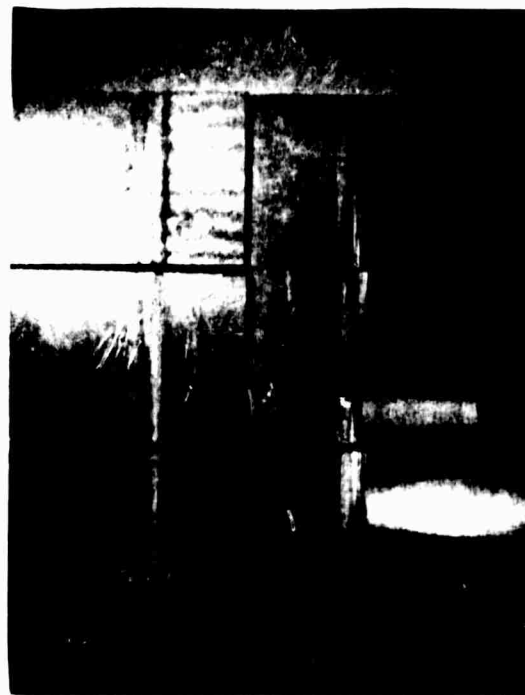
1 A&B

2 A&B

3 A&B



1 RMS NOMINAL, PAPER LAPPED



110 RMS NOMINAL, TURNED

1 A&B

2 A&B

3 A&B



FINE GRAIN, HIGH PRESSURE GRIT BLAST



COARSE GRAIN, HIGH PRESSURE GRIT BLAST

FIGURE 3. BOND FRACTURE SURFACES OF
SELECTED LAP SHEAR SPECIMENS

Most important, however, was this observation:

The bond strength was inversely proportional to the area of the interfacial separation at the initiation site.

That observation fits very well with brittle fracture strengths versus initiation site sizes observed for high strength metals and structural ceramics.

Perhaps more important was the conclusion that bond strength is directly controlled by the interfacial bond condition, rather than bulk adhesive or bulk substrate properties.

Reinspection of the entire listed data, in the light of the above-stated conclusions, provided the foundation for creative inspiration on the part of the author. What if the Thomas Young relationship held throughout the adhesive bonding process with regard to the quantum mechanical bond between cured adhesive and metallic substrate; would the surface free energy state of the adhesive/substrate interface be directly related to bond strength? Through careful derivation and appropriate data analysis the answer was found to be "yes".

2. Prediction of Bond Strength

The ability to mathematically predict adhesive bond strength for practical adhesive bonds is a long-sought-after goal (References 3 and 4). Countless approaches have been tried over the decades with essentially no success whatever. The Science of Adhesion has fallen into a circular path of re-referencing the re-referenced works of the past. My discussion in this section takes advantage of what has already been learned, yet it leads off in a new direction, in hopes of breaking the vicious circle. Adhesive bond strength can be accurately predicted, and in an amazingly straightforward manner.

All paths in the science of adhesion lead back to the Thomas Young equation (1805) which described the equilibrium between the stationary drop of a liquid and the surface of a solid:

$$\gamma_S - \gamma_{LS} - \gamma_L \cos \theta = 0 \quad (4)$$

where: γ_S = solid surface free energy (in vacuum)
 γ_L = liquid surface free energy (in vacuum)
 γ_{LS} = solid-liquid interface surface free energy
 θ = contact angle at three phase point

The physical picture of this "contact angle" relationship is shown in Figure 4. Modifications of this basic relationship have been presented and studied by Dupre', Zisman, Wenzel et al., the main reason being the obvious physical inability to measure γ_{LS} . Their approaches have eliminated γ_{LS} and concentrated on analyzing in terms of γ_L and $\cos \theta$. But take a second look at γ_{LS} . Is this perhaps a case of "throwing the baby out with the bath water?" It certainly is, as we shall see.

$$\gamma_s = \gamma_{Ls} + \gamma_L \cos \theta$$

THOMAS YOUNG EQUATION (1805)

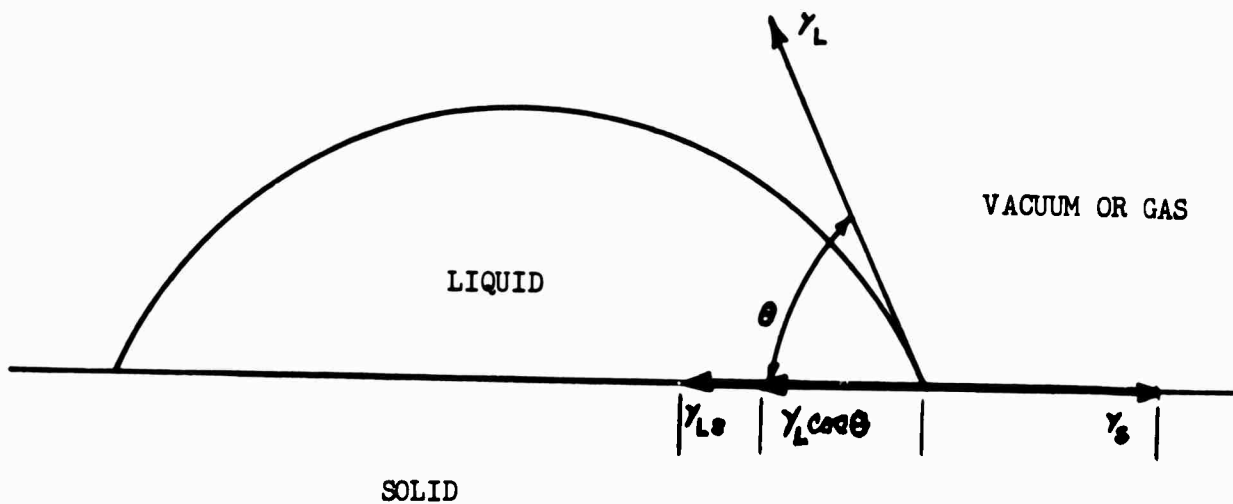


FIGURE 4. FORCE EQUILIBRIUM CONDITION
AT THREE-PHASE POINT FOR A
LIQUID DROPLET ON A SOLID SURFACE

$$\text{BOND STRENGTH} = \frac{\gamma_s - \gamma_L \cos \theta}{\left(\frac{1}{2}\right)(k_o)(\text{BONDLIN THICKNESS})(175127)}$$

ZURBRICK EQUATION FOR PREDICTING BOND STRENGTH

The approach taken here is that γ_{LS} , the surface free energy of the adhesive/substrate interface, is in fact the true value of bond strength. Stated slightly differently, γ_{LS} is the energy that must be added to the bond interface to form a given area of new substrate surface and an equal area of new adhesive surface. Is this the mechanism of observed adhesive bond failure? Yes; and the concept is simplified if we assume that γ_{LS} changes in direct proportion to γ_L as the adhesive changes from liquid to solid through chemical reaction, solvent evaporation, coalescence, etc. This we do not actually know at present, but it is a reasonable assumption that will be borne out.

Quantum mechanics of chemical bonding (See Quarterly Report No. 4 under the subject contract) support the idea that the action of wetting is the formation of substrate/adhesive chemical bonds, each bond exact in the frequency and molecular electron orbitals associated with that bond. The energy required to break one such bond is a fixed value, the total energy being the sum of energy for all bonds broken. Thus the adhesive bond strength is related directly to the number of chemical bonds formed during wetting. Existing bond energies and lengths (bonding, antibonding orbitals) will be modified somewhat by the physical/chemical changes in the bulk adhesive associated with "setting" (liquid to solid transformation) but for "proper" joints this should be minimal. (Bikerman's picture of the "weak boundary layer" is the case of a drastic modification, with time, of these bonds, even to the breaking of some. Although an important aspect, we will consider only the most frequent case where no wetting-assembled bonds are broken or severely changed, or no new bonds are added with time). The Thomas Young equation (4), therefore, contains all the necessary primary variables and fixes their relationship.

Equation (4) can be written as a simple force balance along a line:

$$\gamma_S = \gamma_{LS} + \gamma_L \cos \theta \quad (5)$$

Rearrangement gives:

$$\gamma_{LS} = \gamma_S - \gamma_L \cos \theta \quad (6)$$

a form which best serves this derivation. It says, essentially, adhesive bond strength is directly related to substrate surface free energy less the contact angle cosine component of adhesive surface free energy. For the purposes of analysis each of the four variables can be considered independent of each other except as related in equation (6). Note that γ_L will be a constant of value particular to the liquid of interest, i.e., an adhesive formulation, distilled water. With γ_S and $\cos \theta$ as the independent variables, we see the following general set of relationships:

γ_{SL}	γ_s	γ_L	$\cos \theta$
Low-Low	Low		Low
Med-Low	Med		
High-Low	High		
Low-Med	Low	CONSTANT	Med
Med-Med	Med		
High-Med	High		
Low-High	Low	CONSTANT	High
Med-High	Med		
High-High	High		

Because we expect a wide range of values for both γ_s and $\cos \theta$, (low, med, high) the resultant values of γ_{LS} can vary even more widely, and without definite apparent pattern. The randomness of adhesive bond strength data is well-known, and often cursed, by the concerned technologists in this field. The recent data produced under the subject contract is a case in point. Now we can begin the exact derivation.

Bond strength values obtained through tests on specimens represent the energy stored in the total loaded bond test specimen volume, both substrates and adhesive, at the moment of fracture initiation. This may be seen as follows:

$$\text{Bond strength} = \frac{\text{load at moment of fracture}}{\text{cross sectional area of bonded joint}} = \frac{L}{A}$$

$$\text{Bond strength} = \frac{\text{pounds force}}{\text{square inch}} = \text{psi} \quad (7)$$

$$\text{But: } 1 \text{ lb/in}^2 = 68948 \text{ ergs/cm}^2 = 68948 \frac{\text{dynes}}{\text{cm}^2}$$

$$\text{ergs} = \text{unit of energy; dynes} = \text{unit of force; } 1 \text{ dyne-cm} = 1 \text{ erg}$$

Thus one psi represents the storage of some energy in the volume of material being loaded.

We can then proceed one step further:

For a given substrate material and configuration, which is held essentially constant, the important variable is the adhesive volume; bond strength is then directly related to the energy stored in the adhesive volume at the moment of fracture initiation.

And continuing:

At the moment of fracture, all of the stored energy is used to create the fracture surfaces.

Returning to the definition of surface free energy we see the obvious analog.

$$\begin{array}{lll} \text{bond strength} & \propto & \gamma_{LS} \\ (\text{psi}) & & (\text{ergs/cm}^2) \end{array} \quad (8)$$

The new surfaces created essentially equal the cross-sectional area A, of the bonded joint configuration. For a given joint configuration that area is a constant, for all practical purposes.

It may readily be seen that the thickness dimension of the bondline is the energy storage primary variable.

But energy is stored by straining or displacing a thickness (or lateral or torsional) dimension to a new value, so that total displacement is the number value required for this derivation. Such displacements are extremely small in practical testing situations and are usually not measured. We can obtain empirical values from test data as will be seen later.

Using the linear relationship: (9)

$$\text{Total displacement} = (\text{strain})(\text{bondline thickness})$$

$$\text{strain} = \text{change in dimension/unit dimension}$$

and assuming that strain, k_o , is a constant for a given adhesive, substrate materials and specimen configuration, we can write:

$$\Delta d = (k_o)(d) \quad (10)$$

For a general system:

$$\text{energy available for fracture surface} = A \int_{d_{\min}}^{d_{\max}} \sigma d(d)$$

$$\begin{array}{ll} \text{where } \sigma = & \text{stress} \\ d = & \text{thickness dimension, apparent} \\ A = & \text{joint area} \end{array}$$

Where the stress-strain relationship is linear over the full loading experience:

$$\text{energy} = \frac{1}{2} (\sigma_{\max})(\Delta d)(A) \quad (11)$$

combining equation (11) with (10) obtain:

$$\text{energy} = \left(\frac{1}{2}\right)(\text{ultimate bond strength})(k_o)(d)(A) \quad (12)$$

where psi and inch dimensions are involved:

$$\text{energy} = (\text{lb})(\text{inch})$$

To convert these units to those familiar in the science of adhesion:

$$\frac{\text{energy}}{A} = \frac{1}{2} (\text{ultimate bond strength})(k_o)(d) \quad (13)$$

lb/inch

$$1 \text{ lb/in} = (1 \text{ lb/sq in})(1 \text{ inch})$$

$$1 \text{ lb/in} = (68948 \text{ dynes/cm}^2)(1 \text{ inch})\left(\frac{2.54 \text{ cm}}{1 \text{ inch}}\right)$$

$$1 \text{ lb/in} = 175127 \text{ dynes/cm or ergs/cm}^2$$

Putting it all together gives us.

$$\gamma_{LS} = \left(\frac{1}{2}\right)(\text{ULT Bond Strength})(d)(175127)(k_o) \quad (14)$$

(ergs/cm²) (psi) (inch) $\frac{\text{ergs/cm}^2}{\text{lb/in}}$

We now have a good first approximation of the relationship between interfacial surface free energy and bond strength.

Going back to Thomas Young's relationship

$$\gamma_{SL} = \gamma_S - \gamma_L \cos \theta \quad (6)$$

and substituting

$$\left(\frac{1}{2}\right)(\text{UBS})(k_o)(d)(175127) = \gamma_S - \gamma_L \cos \theta \quad (15)$$

$$\text{UBS} = \frac{\gamma_S - \gamma_L \cos \theta}{\left(\frac{1}{2}\right)(k_o)(d)(175127)} \quad (16)$$

This equation provides the means to predict bond strength if we can non-destructively measure: d, bondline thickness

θ, contact angle

γ_S, substrate surface free energy

when:

1. γ_L is known
2. k_o is a known and constant
3. integral for stress-strain curve is known

Note that bond strength is inversely proportional to bondline thickness, which has been reported in the literature on numerous occasions.

In order to evaluate k_o and predict individual γ_s values from specimen test data we use equation (16) in this rearrangement:

$$\gamma_s = \gamma_L \cos \theta + \left(\frac{1}{2}\right)(UBS)(k_o)(d)(175127) \quad (17)$$

and for k_o

$$k_o = \frac{\gamma_s - \gamma_L \cos \theta}{\left(\frac{1}{2}\right)(UBS)(d)(175127)} \quad (18)$$

Using these values for a butt tensile specimen configuration:

$$\gamma_s = 200 \text{ ergs/cm}^2 \text{ (estimated)}$$

$$\gamma_L = 72.8 \text{ ergs/cm}^2 \text{ (distilled water)}$$

$$\theta = 5^\circ$$

$$\cos \theta = 0.996$$

$$UBS = 5000 \text{ psi}$$

$$d = 0.006 \text{ inch}$$

$$\text{calculated } k_o = 0.0000486, \approx 0.00005$$

$$\text{apparent displacement} = (5 \times 10^{-5})(0.006 \text{ inch}) = 3 \times 10^{-6} \text{ inch}$$

$$= 3 \mu \text{ inches}$$

Using a γ_s value of 200 ergs/cm² and values from the data for butt tensile, core shear, and lap shear specimens listed, these apparent values of strain were obtained:

$$\text{butt tensile } k_o = 0.500 \times 10^{-4}$$

$$\text{core shear } k_o = 0.833 \times 10^{-4}$$

$$\text{lap shear } k_o = 4.000 \times 10^{-4}$$

The exact calculations for γ_{LS} and γ_s using the experimental data are given in Tables I, II, and III. The summarized data in Tables IV, V, and VI, shows the relationship between method of surface generation and substrate surface free energy, as prepared and after etch. These results have verified the analytical approach and provide the incentive to develop and refine it further.

TABLE I

Calculation of Surface Free Energies

Specimen Type: BUTT TENSILE $k_0 = 0.500$ $\gamma_L = 72.8 \text{ ergs/cm}^2$

Code	Specimen 1A			Specimen 2A			Specimen 3A			Average γ_{Lg} ergs/cm ²
	Bond Strength psi	Bondline Thickness inch	γ_{Lg} ergs/cm ²	Bond Strength psi	Bondline Thickness inch	γ_{Lg} ergs/cm ²	Bond Strength psi	Bondline Thickness inch	γ_{Lg} ergs/cm ²	
1	3900	.0055	93.91	3750	.0038	62.39	3200	.0049	66.65	74.95
5	5770	.0044	111.15	4780	.0042	87.90	5520	.0044	106.72	101.92
7	3600	.0100	157.61	3920	.0047	80.66	5190	.0067	152.24	130.17
10	4100	.0071	127.45	5040	.0066	145.64	2660	.0042	48.91	107.33
20	5580	.0076	185.67	6930	.0065	197.21	4750	.0055	114.38	165.75
40	4070	.0061	108.70	3920	.0065	111.56	4240	.0052	96.53	105.60
80	5300	.0047	109.06	4210	.0064	117.97	5100	.0067	149.60	125.54
110	4450	.0083	161.71	4080	.0075	133.97	3630	.0081	128.73	141.47
150	5750	.0077	193.54	5510	.0049	115.21	5320	.0060	139.75	150.60
FGLP	7590	.0061	202.71	5210	.0056	127.74	7300	.0045	143.82	158.09
FGHP	6930	.0060	200.25	7160	.0058	181.88	5560	.0055	133.88	171.98
CCLP	5110	.0073	163.32	6720	.0060	176.53	4710	.0046	94.86	144.90
CGHP	6110	.0044	117.70	5760	.0047	68.09	6770	.0053	157.09	114.29

TABLE I (Continued)

Code	Cos θ		Max (M)		Max (E)		Min (M)		Min (E)		CLA (M)		CLA (E)	
	Max	Min	Max	Min	Max	Min	Max	Min	Max	Min	Max	Min	Max	Min
			γ_S	γ_S	γ_S	γ_S	γ_S	γ_S	γ_S	γ_S	μ	μ	μ	μ
			Max	Min	Max	Min	Max	Min	Max	Min	Max	Min	Max	Min
1	.31730	.70091	95.05	120.01	.93012	.95769	142.71	146.88	1.2	10.0				
5	.15224	.51112	115.19	141.19	.90631	.95629	167.90	173.72	6.0	14.0				
7	.13053	.60876	139.67	174.49	.97630	.96363	201.24	200.32	9.2	15.0				
10	.11320	.58779	115.57	150.12	.98769	.98902	179.23	179.33	14.4	24.0				
20	.34202	.80902	190.65	221.65	.97630	.97237	236.82	236.54	7.0	14.0				
40	.44620	.94552	138.08	174.43	.99756	.99619	178.22	178.12	37.5	35.0				
80	.19937	.73135	140.05	178.78	.97630	.99540	196.61	198.01	63.0	45.0				
110	.16505	.84339	153.49	202.87	.95372	.99027	210.90	213.56	62.0	60.0				
150	.11320	.68835	158.84	200.71	.89101	.97815	215.47	221.21	84.0	77.0				
FGLP	.55919	.71325	198.80	210.01	.93969	.98629	226.50	229.89	22.0	25.0				
FGHP	.55919	.51540	212.69	209.50	.93969	.985 est	240.39	243.69	29.0	50.0				
CGLP	.24192	.55070	162.51	187.17	.96363	.98325	215.05	216.48	31.0	30.0				
CGHP	.20791	.76041	129.43	169.65	.97437	.98769	155.22	155.19	55.0	70.0				

TABLE II

Calculation of Surface Free Energies

Specimen Type: CORE SHEAR $k_o = 0.833$ $\gamma_L = 72.8 \text{ ergs/cm}^2$

Code	Specimen 1A			Specimen 2A			Specimen 3A			Average γ_{Lg} ergs/cm ²
	Bond Strength psi	Bondline Thickness inch	γ_{Lg} ergs/cm ²	Bond Strength psi	Bondline Thickness inch	γ_{Lg} ergs/cm ²	Bond Strength psi	Bondline Thickness inch	γ_{Lg} ergs/cm ²	
1	3140	.0057	130.55	4500	.0048	157.55	460	.0042	14.09	100.73
5	1280	.0055	51.35	1470	.0063	67.55	2870	.0046	96.30	71.73
7	1610	.0052	61.07	1590	.0049	56.83	4530	.0039	128.86	62.25
10	2310	.0051	85.93	3600	.0036	94.53	3610	.0050	131.66	104.04
20	2800	.0063	128.67	4370	.0097	309.19	1000	.0074	53.98	163.95*
40	2440	.0088	156.62	2940	.0082	175.84	3040	.0079	175.17	169.21
80	2320	.0074	125.22	4710	.0055	188.95	1250	.0052	47.41	120.53
110	3280	.0056	133.98	2000	.0052	75.86	590	.0082	35.29	81.71
150	1610	.0060	70.46	2470	.0075	135.12	1800	.0064	84.03	96.54
FGLP	4440	.0081	262.33	4160	.0066	200.27	1400	.0058	59.23	173.94
FGHP	1540	.0055	61.78	5150	.0046	172.80	4260	.0049	152.26	128.95
CGLP	5250	.0060	229.76	4770	.0073	253.99	4730	.0057	196.65	226.80
CGHP	5480	.0039	155.89	5270	.0054	207.57	5070	.0040	147.92	170.46

* Wide range

TABLE III

Calculation of Surface Free Energies

Specimen Type: LAP SHEAR $k_o = 4.000$ $\gamma_L = 72.8 \text{ ergs/cm}^2$

Code	Specimen 1A			Specimen 2A			Specimen 3A			Average γ_{LS} ergs/cm ²
	Bond Strength psi	Bondline Thickness inch	γ_{LS} ergs/cm ²	Bond Strength psi	Bondline Thickness inch	γ_{LS} ergs/cm ²	Bond Strength psi	Bondline Thickness inch	γ_{LS} ergs/cm ²	
1	1360	.0021	100.03	1320	.0039	180.31	910	.0027	86.06	122.13
5	1260	.0026	114.74	1390	.0010	48.69	910	.0032	101.99	88.47
7	1240	.0050	217.16	1320	.0020	92.47	1140	.00131	52.31	120.65
10	1160	.0012	48.76	1280	.0023	103.11	1080	.0035	132.40	94.76
20	950	.0039	135.23	1200	.0031	130.29	1120	.0019	74.53	113.35
40	1000	.0045	157.61	1000	.0046	161.12	822	.0036	103.65	140.79
60	1130	.0072	284.97	1060	.0061	226.47	830	.0044	127.91	213.12
110	940	.0036	115.53	970	.0059	200.45	760	.0064	170.36	163.11
150	750	.0050	150.61	1120	.0027	105.92	770	.0028	75.51	110.68
FGLF	975	.0037	126.35	940	.0044	144.87	975	.0039	133.18	134.80
FGHP	1050	.0037	136.07	1040	.0030	109.28	1060	.0048	178.21	141.19
CGLF	925	.0082	71.27	1230	.0013	56.01	1170	.0027	111.59	79.63
CGHP	1230	.0030	129.27	965	.0052	175.70	1130	.0053	209.77	171.59

TABLE III (Continued)

Code	Cos θ		Max (M) γ_s^2 ergs/cm ²		Max (E) γ_s^2 ergs/cm ²		Cos θ		Min (M) γ_s^2 ergs/cm ²		Min (E) γ_s^2 ergs/cm ²		CLA (M) μ in	CLA (E) μ in
	Max (M)	Max (E)	Cos θ	Max (M)	Max (E)	Cos θ	Min (M)	Min (E)	Cos θ	Min (M)	Min (E)	Cos θ	Min (M)	Min (E)
1	.40674	.34202		151.74	147.03		.93042	.97630		189.86	193.20		1.2	7.0
5	.05234	.27564		92.28	106.54		.80902	.94552		147.37	157.30		4.5	7.0
7	.34202	.43837		145.55	152.56		.96363	.99255		190.80	192.91		7.2	9.0
10	.46947	.19061		128.94	108.65		.94552	.98325		163.59	166.34		8.5	11.0
20	.35837	.46947		139.44	147.53		.94264	.96126		181.97	183.33		17.0	32.0
40	.25882	.91706		159.63	207.55		.97030	.99141		211.43	212.97		21.0	22.0
80	.45399	.55919		246.17	253.83		.90631	.97237		279.10	283.91		37.0	32.0
110	.39875	.95630		192.14	232.73		.89493	.99905		228.26	235.84		47.0	58.0
150	.19081	.06976		124.57	115.76		.92718	.94552		176.18	179.51		72.0	72.0
FGLP	.52250	.27564		172.84	154.87		.98325	.94832		206.38	203.84		20.0	20.0
FGHP	.77715	.44620		197.77	173.67		.97030	.96593		211.83	211.51		32.5	45.0
CGLP	.14781	.97437		90.39	150.56		.95106	.99863		148.87	152.33		34.0	36.0
CGHP	.11320	.03490		179.83	174.13		.90631	.85717		237.57	233.99		55.0	60.0

TABLE IV

SPECIMEN TYPE: BUTT TENSILE

CALCULATED SURFACE FREE ENERGIES

NOMINAL ROUGHNESS	γ_{LS} AVERAGE	γ_s MAX (M)	γ_s MAX (E)	γ_s MIN (M)	γ_s MIN (E)	PREPARATION PROCESS
RMS inch	ergs/cm ²	ergs/cm ²	ergs/cm ²	ergs/cm ²	ergs/cm ²	
1	75	98	126	143	147	Paper lapped
5	102	115	161	168	174	Paper lapped
7	130	140	174	201	200	Paper lapped
10	107	116	150	179	179	Paper lapped
20	166	191	225	237	237	Turned
40	106	138	174	178	178	Paper sanded
80	126	140	179	197	198	Turned
110	141	153	203	211	214	Turned
150	151	159	201	215	222	Turned
FGLP	158	199	210	227	230	Grit Blast
FGHP	171	213	210	240	244	Grit Blast
CGLP	145	163	187	215	216	Grit Blast
CGHP	114	129	170	185	186	Grit Blast

TABLE V

SPECIMEN TYPE: CORE SHEAR

CALCULATED SURFACE FREE ENERGIES

NOMINAL ROUGHNESS	γ_{LS} AVERAGE	γ_s MAX (M)	γ_s MAX (E)	γ_s MIN (M)	γ_s MIN (E)	PREPARATION PROCESS
RMS inch	ergs/cm ²	ergs/cm ²	ergs/cm ²	ergs/cm ²	ergs/cm ²	
1	101	103	167	153	173	Paper lapped
5	72	92	142	142	144	Paper lapped
7	82	94	151	152	155	Paper lapped
10	104	127	168	174	176	Paper lapped
20	164	185	228	235	236	Paper sanded
40	169	187	235	240	242	Paper sanded
80	121	136	183	192	193	Paper sanded
110	82	103	143	150	154	Turned
150	97	118	154	167	169	Turned
FGLP	174	219	246	245	247	Grit Blast
FGHP	129	178	202	199	202	Grit Blast
CGLP	227	262	299	296	300	Grit Blast
CGHP	170	188	243	243	243	Grit Blast

TABLE VI
SPECIMEN TYPE: LAP SHEAR

CALCULATED SURFACE FREE ENERGIES

NOMINAL ROUGHNESS RMS inch	γ_{LS} AVERAGE ergs/cm ²	γ_s MAX (M) ergs/cm ²	γ_s MAX (E) ergs/cm ²	γ_s MIN (M) ergs/cm ²	γ_s MIN (E) ergs/cm ²	PREPARATION PROCESS
1	122	152	147	190	193	Paper lapped
5	88	92	109	147	157	Paper lapped
7	121	146	153	191	193	Paper lapped
10	95	129	109	164	166	Paper lapped
20	113	139	148	182	183	Paper sanded
40	141	160	208	211	213	Turned
80	213	246	254	279	284	Turned
110	163	192	233	228	236	Turned
150	111	125	116	178	180	Turned
FGLP	135	173	155	206	204	Grit Blast
FGHP	141	198	174	212	212	Grit Blast
CGLP	80	90	151	149	152	Grit Blast
CGHP	172	180	174	238	234	Grit Blast

B. Nondestructive Surface Characterization

1. Definitive Direction

Until recently the concept of surface characterization has been general in scope, with little exact definition as to what factors provide the necessary information. Results of the Surface Condition Study, particularly the predictive equation for bond strength, have brought this situation into clearer focus. It is now apparent that three units of information are required:

1. Surface free-energy state of substrates
2. Contact angle, referenced to distilled water or actual liquid adhesive
3. Bondline thickness

The first two are sufficient to characterize the substrate surface prior to bonding. The third is obtained from the completed adhesive joint (Non-destructive test techniques are currently available or adaptable for measuring bondline thicknesses).

Great impetus has been added, therefore, to pursuing nondestructive test methods and techniques which specifically measure and correlate with surface free-energy state and contact angle. The measurement of contact angle, employing electronic sensing of changes in a liquid droplet, appears reasonably straightforward. The independent measurement of surface-free-energy state has been, and continues to be, the primary challenge of the subject contract.

The "Zurbrick equation for predicting bond strength" provided the means to back-calculate (equation (17) from experimental data to substrate surface free energy values. These values in turn allowed the selection of prepared substrates (remaining four from originally prepared 10, for each of 13 different surfaces, for three specimen types) to cover a wide range of γ_s values. For convenience the core shear substrates were chosen, and three sets of four selected:

Substrate	Calc'd γ_s ergs/cm ²
5 RMS Nominal	92
20 RMS Nominal	185
CGLP Grit Blast	262

These γ_s values were used in the correlation and analysis of nondestructive test raw output data during technique feasibility studies.

2. Gas-phase Ultrasonic Transmission Method

An extensive feasibility study of the gas-phase ultrasonic transmission method has been completed. Results have shown that characteristic acoustic waves are emitted by substrate surfaces and that these may be readily detected and analyzed. Frequency domain analysis has revealed that new frequencies (1.275, 1.325, 1.350 MHz) arise as a result of specimen (core shear) insertion into the acoustic field. Additional frequencies, especially the higher harmonics, arise

at low amplitudes corresponding to variations in surface energetic character. Test conditions were sufficiently stable to provide reproducible response signatures. This work encourages development of techniques directed toward isolating the surface energy characteristic frequencies for correlations with calculated surface free energy values.

The equipment and system used in the feasibility study are presented in Figure 5. A holding fixture was prepared for a fixed transmitting transducer (Automation Industries Type 57A3641, 2" dia, 1.0 MHz) and an adjustable receiving transducer (Budd Co. Model 4CWC, 1/2" dia, 1.0 MHz). The fixture and transmitter were placed in a tub of water such that the water surface reached approximately half way up a core shear specimen. The specimen rested on a cork pad over an 11/16" diameter aperture. Specimen surface to receiver distance was 7/16 inch. Photographs of the analyzer traces were obtained for comparison and frequency data reduction.

3. Electric Field Reflectometry

A feasibility study of electric field reflectometry at 1.0 KHz has been completed. Results have shown that probe capacitance values show correspondence to surface energy state. The equipment used is presented in Figure 6. A 1/4 inch square, "polarized" probe having a nominal depth of field of .032" was positioned near, but not touching, the substrate surface. Probe capacitance and dissipation values were obtained. The difference between "empty" probe value and "full" probe value was compared with calculated surface free energies for the three trial substrates.

This work encourages development of capacitance probes specifically designed for surface energy measurements, and particularly suited to a hand scanning inspection technique.

III CONCLUSIONS AND RECOMMENDATIONS

1. Conclusions

- a. An equation for predicting adhesive bond strength, based upon the Thomas Young relationship, has been developed. It is proposed to the adhesive bonding community for critique, confirmation, and practical use.

2. Recommendations

None

IV. FUTURE WORK PLANNED

The following work is planned for the quarter 1970 April 20 through 1970 July 19:

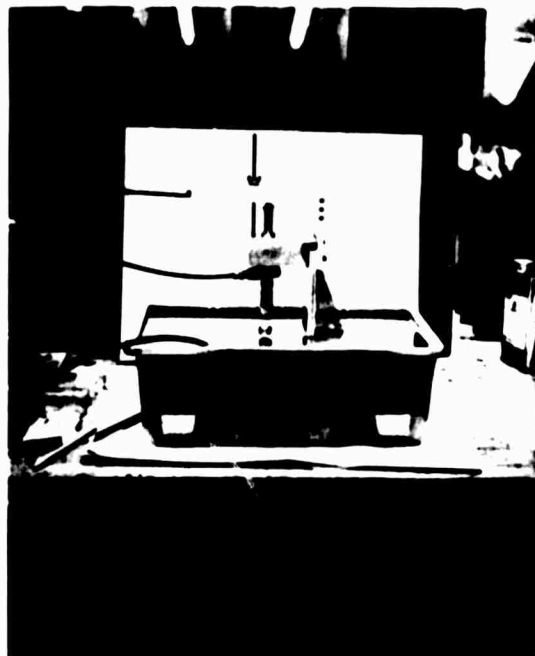
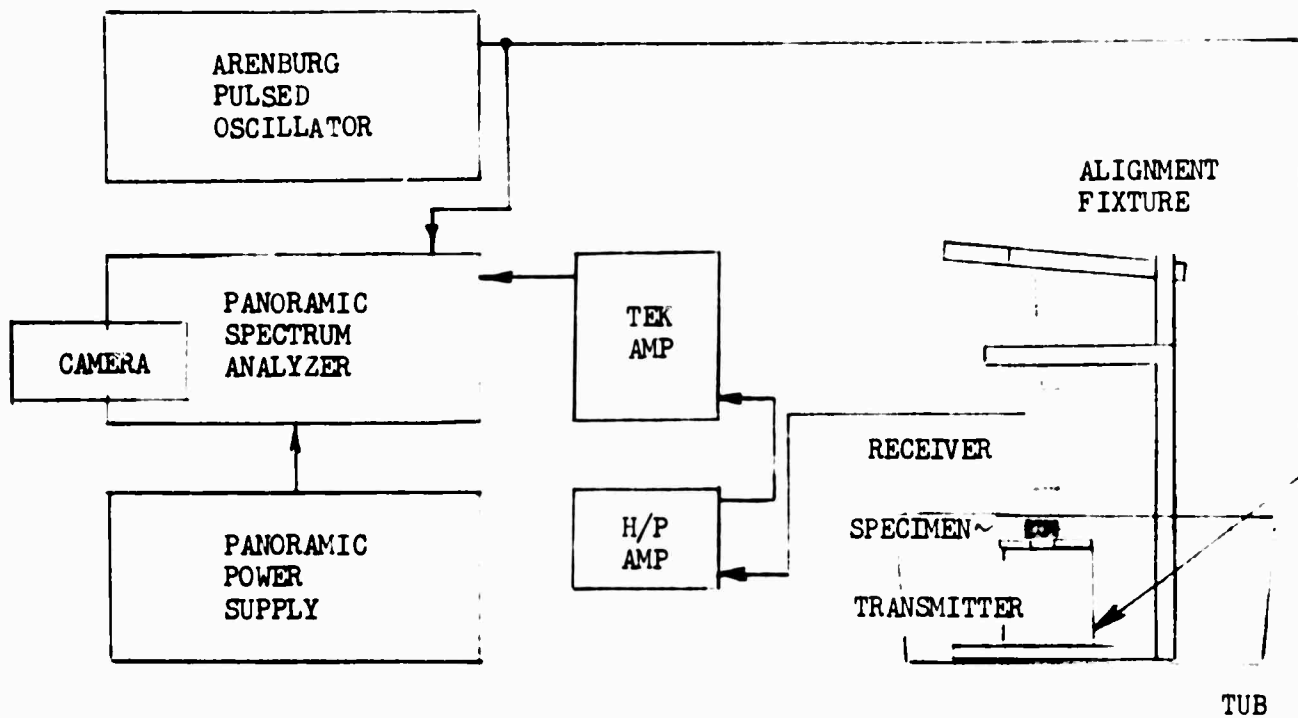


FIGURE 5. GAS-PHASE ULTRASONIC TRANSMISSION METHOD FEASIBILITY STUDY EQUIPMENT AND SYSTEM

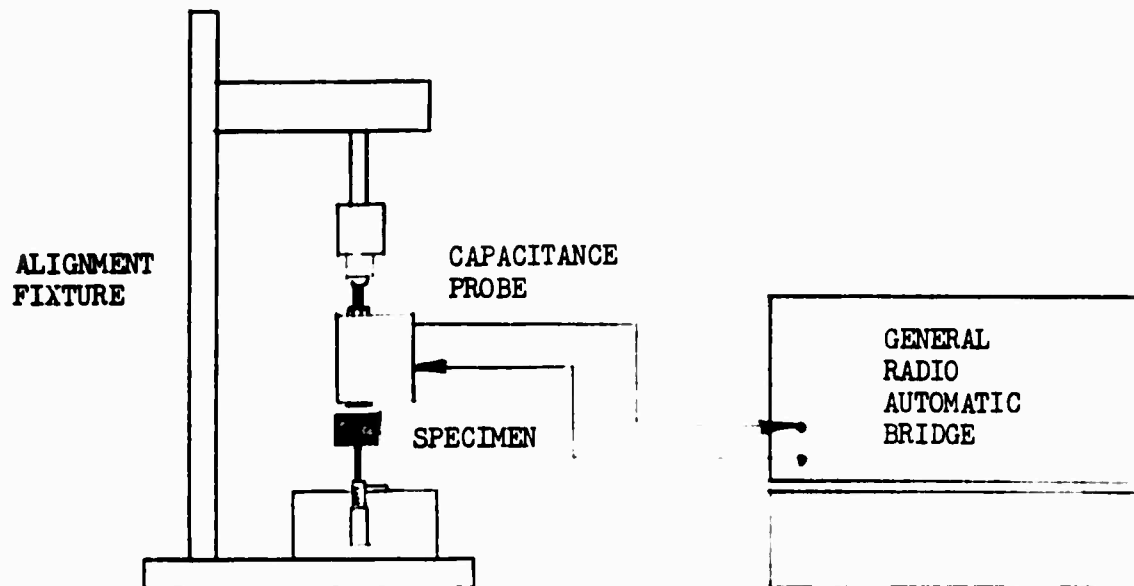

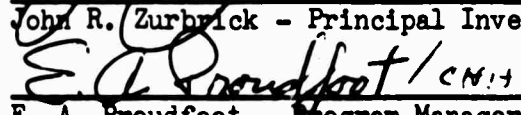


FIGURE 6. ELECTRIC FIELD REFLECTOMETRY METHOD FEASIBILITY STUDY EQUIPMENT AND SYSTEM (1.0 KHZ)

1. Complete feasibility studies for electric field reflectometry techniques.
2. Investigate alternative surface characterizing techniques for causal relationships.
3. Write and deliver final technical report for the currently funded year of investigation.



John R. Zurbrich - Principal Investigator



E. A. Proudfoot - Program Manager

REFERENCES

1. Marian, J. E., "Surface Texture in Relation to Adhesive Bonding," Symposium on Properties of Surfaces, ASTM Materials Science Series -4, ASTM STP-340, American Society for Testing and Materials (1963) pp 142-144.
2. Hughes, E. J., and Rutherford, J. L., "Study of Micromechanical Properties of Adhesive Bonded Joints," Technical Report No. 3744, General Precision Systems, Inc., Little Falls, N. J. (August 1968) (AD 673745).
3. "Sharp Receives Adhesive Age Award at Houston D-14 Meeting", Adhesives Age Vol 11, No 5, (May 1968), pp 42-44.
4. McClung, R. W., Oliver, R. B., and Rowand, R. R., "Section IV Technical Problem Areas" Nondestructive Testing, Publication NMAB-252, National Materials Advisory Board, NRC (June 1969)